

Domain wall formation at the $c(2\times 2)$ - (2×1) phase transition of the CdTe(001) surface

H. Neureiter,¹ S. Tatarenko,² S. Spranger,¹ and M. Sokolowski^{1,*}

¹Experimentelle Physik II, Universität Würzburg, Am Hubland, D-97074 Würzburg, Germany

²Laboratoire de Spectrométrie Physique, CNRS, Université J. Fourier, Boîte Postale 87, 38402 Saint-Martin d'Hères, France

(Received 18 February 2000)

A specific type of line defect was detected at the temperature-driven $c(2\times 2)$ - (2×1) phase transition of the CdTe(001) surface, the formation of *parallel domain walls* in the (2×1) phase, using high-resolution low-energy electron diffraction. The domain walls arise because of spontaneous ordering of Cd surface vacancies in the Cd-terminated top layer and yield an effective relaxation of surface strain. Their general relevance for structural and thermodynamic properties of (001) semiconductor surfaces is discussed.

The structures of polar (001) surfaces of binary and multiple-element semiconductor materials [e.g., InAs,¹ CdTe,² and GaAs (Ref. 3)] are of considerable interest because of fundamental aspects and because of their technological relevance for optoelectronic devices. One important issue is to understand the relation between structural properties on the one hand and stoichiometric and thermodynamic parameters on the other. In particular for the GaAs(001) surface, a number of experimental studies have been directed at the atomic details of the surface reconstructions and have related them to theoretical energy calculations partially performed from the *ab initio* level. One specific aspect of this approach is that energy differences between different ideal surface reconstructions may be only small,⁴ and therefore structural defects of the reconstructions, e.g., surface vacancies or antiphase boundaries, may become relevant. For instance, the importance of Ga vacancies in the second layer was recently deduced for the $\beta(2\times 4)$ phase of GaAs(001) grown by molecular-beam epitaxy (MBE).³

Whereas many investigations have been performed at room temperature, only a few experiments have considered the structures and the phase transitions between them at elevated temperatures (e.g., Refs. 3 and 5). Nonetheless, the details of these are of equal importance, e.g., for the optimization and understanding of MBE growth, as well as the basic aspects concerning surface phase transitions of multiple-element semiconductors. For the latter, interesting phenomena may arise from small variations of the surface stoichiometry of the constituent elements. In this work, we have investigated the temperature-driven $c(2\times 2)$ - (2×1) phase transition of the Cd-terminated CdTe(001) surface⁵ by high-resolution low-energy electron diffraction (HRLEED). We observe a splitting of the HRLEED spot profiles for the (2×1) phase, which indicates spontaneous formation of parallel domain walls. Such defects have not been noted so far and presumably this has general implications for the understanding of polar semiconductor (001) surfaces from energetic and thermodynamic viewpoints.

In comparison to III-V semiconductors, II-VI (001) surfaces exhibit less complex reconstructions. For the CdTe(001) surface considered, there exists a well-defined structural model for the low-temperature $c(2\times 2)$ phase, which is based on x-ray diffraction results⁶ and supported by scanning tunneling microscopy⁷ (STM) and surface core-

level shifts (SCLS's) in photoemission data.⁸ The $c(2\times 2)$ structure is formed by half a monolayer (ML) of Cd atoms in the top layer (Fig. 1). The overall important structural feature is a strong inward relaxation of the terminal Cd atoms, bringing them down to only 0.07 Å above the first Te layer, which reduces the surface dipole. The second-layer Te atoms are horizontally pushed away along the $[1\bar{1}0]$ direction into the Cd vacancies, leading to a rotation of the Te bonds to the Cd atoms in the third layer. This type of reconstruction is believed to relax the surface strain most effectively.⁶

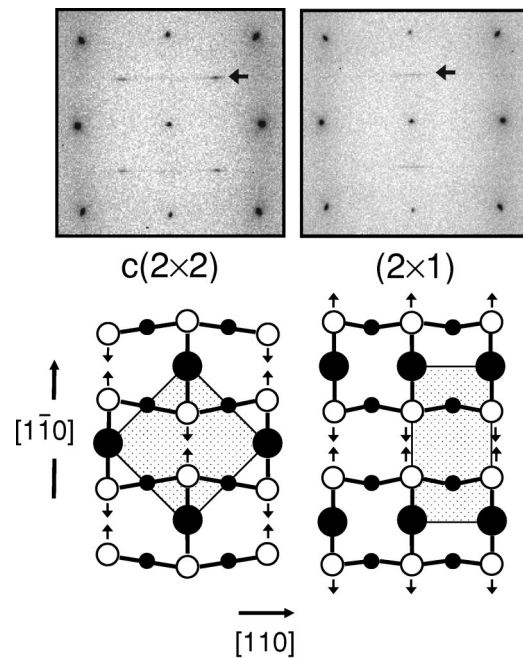


FIG. 1. (Top) LEED patterns of the Cd(001) surface at 250 °C (left) and 300 °C (right) for 33.8 eV electron energy. The arrows mark the positions of the superstructure spots from the reconstructions. (Bottom) Hard-sphere models of the corresponding ideal $c(2\times 2)$ and (2×1) surface reconstructions with primitive unit cells indicated. The horizontal displacements of the top-layer Cd atoms from the bulk positions are indicated. Note that the (2×1) structure can be transformed into the $c(2\times 2)$ structure by a shift of every second row of Cd atoms along the $[1\bar{1}0]$ direction. Larger and smaller filled circles denote Cd atoms of the first and third layer, and open circles represent second-layer Te atoms.

The (2×1) reconstruction at high temperatures (Fig. 1) has so far not been subject to a detailed structural investigation. From temperature-dependent Auger measurements (see below), however, the same surface termination (0.5 ML Cd) as for the $c(2\times 2)$ is deduced for the ideal (2×1) reconstruction. The temperature-driven $c(2\times 2)$ - (2×1) phase transition was identified as a *first-order* phase transition⁵ from its hysteresis, in accordance with expectations from Landau rules.⁹ On top of the aforementioned issues, this phase transition is of interest, since from *ab initio* calculations the energetic difference of the two structures is expected to be only very small, i.e., of the order of 0.02 eV per (1×1) unit cell.⁴

The experiments were performed in ultrahigh vacuum on the (001) surface of a nominally nondoped CdTe(001) crystal, purchased from Japan Energy Corporation. A clean surface with large terraces of up to 1000 Å was prepared by Ar-ion sputtering and subsequent annealing at about 300 °C. Photoemission SCLS measurements showed that the Cd-terminated surface is obtained by this preparation route.⁸ Temperatures were measured by a thermocouple in direct contact with the sample holder. The transfer width of the commercial HRLEED instrument was about 1800 Å.¹⁰

Auger intensities were measured for the Cd_{MNN} (376 eV) and Te_{MNN} (483 eV) peaks with a cylindrical-mirror analyzer in the differential mode ($E_0 = 3$ keV). For calculation of the Cd coverage (θ_{Cd}) in the top layer we used the layer model¹¹ and an inelastic mean free path of 13.5 Å for Cd and Te layers.¹⁰ For the Cd-terminated surface considered here (with a complete Te layer as the second layer), the layer model yields a correlation of the ratio of the Auger intensities ($[\text{Cd}_{MNN}]/[\text{Te}_{MNN}]$) and the Cd coverage that is approximately linear: $[\text{Cd}]/[\text{Te}] = (I_{\text{Cd}}^\infty/I_{\text{Te}}^\infty)[3.1\theta_{\text{Cd}}(\text{ML}) + 0.85]$.¹² Here $I_{\text{Cd}}^\infty/I_{\text{Te}}^\infty$ denotes the ratio of the Auger sensitivity factors. For absolute Cd coverages, $I_{\text{Cd}}^\infty/I_{\text{Te}}^\infty$ was calibrated to 1.65 from the structural model of the surface at 270 °C (see below).

Figure 1 displays two typical HRLEED patterns of the surface, which were taken at temperatures just below (250 °C) and above (300 °C) the phase transition, showing clearly the $c(2\times 2)$ and (2×1) superstructure spots, respectively. The phase transition between the two structures occurs at 270 ± 10 °C. This can be derived from Fig. 2(a), in which the integrated intensities of the superstructure spots [numerically obtained from one-dimensional (1D) spot profiles] are plotted as a function of temperature. As expected for a first-order phase transition, the $c(2\times 2)$ superstructure spots vanish at the transition without further broadening, which would be significant for a second-order phase transition.⁹

From Fig. 1 one observes that the $c(2\times 2)$ spots are elongated along the $[110]$ direction. This effect is due to antiphase boundaries between $c(2\times 2)$ domains along the $[1\bar{1}0]$ direction, partially caused by Cd vacancies on this surface, i.e., a deficiency of Cd in the top layer compared to 0.5 ML.¹⁰ Experimental evidence for these Cd vacancies is given by (i) SCLS photoemission data,⁸ (ii) the fact that the intensity of the $c(2\times 2)$ spots can be enhanced by additional Cd dosing,¹² and (iii) STM measurements.¹³ The last reveal that at room temperature small (2×1) domains, pinned at

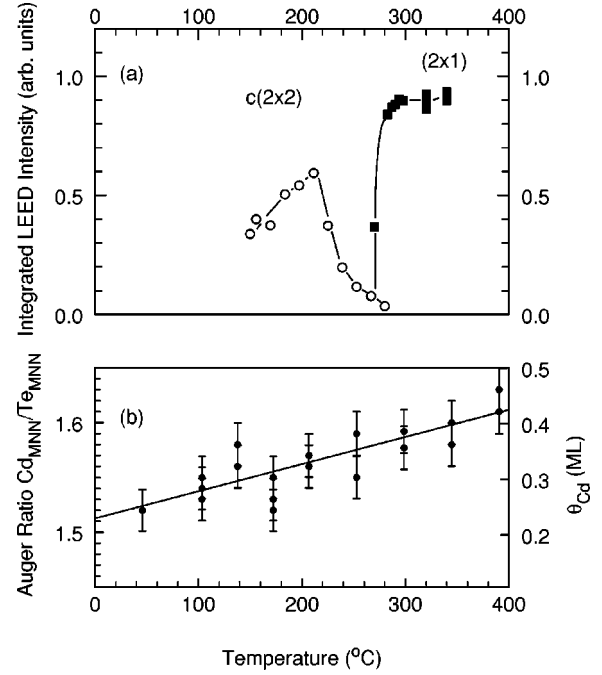


FIG. 2. Integrated intensities of the $c(2\times 2)$ and (2×1) superstructure LEED spots (a) and the Cd_{MNN} to Te_{MNN} Auger peak-to-peak intensity ratio and Cd coverage (θ_{Cd}) in the top layer derived from the Auger data (b) as a function of temperature. Solid lines are guidelines to the eye.

Cd vacancies, coexist with the $c(2\times 2)$ structure. We note that the rise of the $c(2\times 2)$ spot intensity in Fig. 2(a) on approaching 200 °C from low temperatures is due to depinning and vanishing of these (2×1) domains.¹⁰

Figure 2(b) shows the Cd/Te Auger ratio and the Cd coverage (θ_{Cd}) as functions of temperature. Between room temperature and 350 °C a reversible increase of θ_{Cd} with temperature from 0.25 to 0.40 ML is detected, which indicates a reduction of the Cd deficiency at higher temperatures. We note that this Cd increase clearly rules out the possibility of a Te-terminated (2×1) phase above 270 °C, discussed earlier,¹⁴ since this would imply a decrease of the Cd/Te Auger ratio at higher temperatures.

The reversible change of the Cd surface coverage as a function of temperature is understood from the fact that the bulk serves as a particle reservoir that allows the surface stoichiometry to adopt a value according to the requirement of the chemical potential of the surface. Especially at higher surface temperatures, this is easily possible, since congruent sublimation of Cd and Te also starts at about 270 °C,¹⁵ i.e., the temperature of the phase transition. Therefore the (2×1) phase is formed on a sublimating surface in a quasidynamic equilibrium. As a consequence, the (2×1) reconstructed surface investigated here corresponds to the thermodynamic-equilibrium surface under UHV, and thus differs from those surfaces prepared under external flux at this temperature by MBE and subsequent quenching.⁵

As can be seen in Fig. 2(a), the intensity of the (2×1) superstructure spots rises very sharply above the transition temperature within only about 20 K. However, the HRLEED pattern of the (2×1) phase (Fig. 1) already indicates that the superstructure spots of the (2×1) phase are considerably

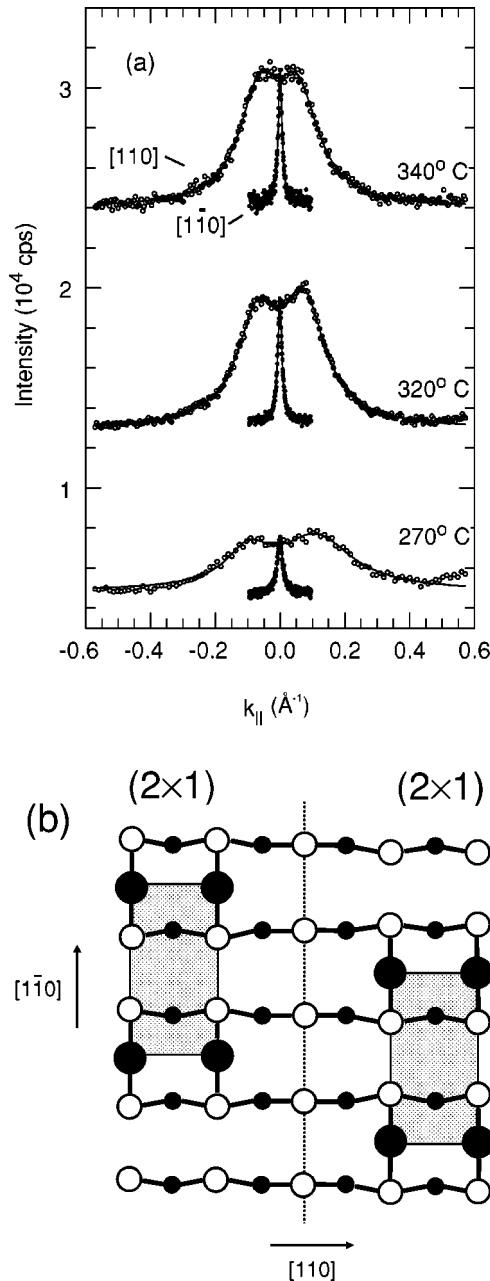


FIG. 3. (a) Line scans of the first-order (2×1) diffraction spots along the $[110]$ and $[1\bar{1}0]$ directions as a function of temperature. The solid lines are fits to the data as described in the text. (b) Schematic hard-sphere model of domain walls (dashed line) between (2×1) ordered domains. Cd and Te atoms are denoted as in Fig. 1.

broadened in the $[110]$ direction. These spot profiles were investigated in detail by 1D line scans. Three profiles of the $(0, \frac{1}{2})$ superstructure spot at different temperatures (see the arrow in Fig. 1), scanned along the $[110]$ and $[1\bar{1}0]$ directions, are displayed in Fig. 3(a). Remarkable is the pronounced splitting into two symmetric and broad peaks of the profiles along the $[110]$ direction. Both the size of the splitting and the width of the two peaks are reduced reversibly by a factor of about 2 from 270 to 340 °C. Quite differently, the profiles along the $[1\bar{1}0]$ direction are very sharp and constant in width, which indicates a large correlation length (300–450 Å) of the (2×1) domains in this direction.

It is noteworthy that no indications of such profile splitting were observed for the (1×1) or $c(2 \times 2)$ spots. An explanation of this effect by parallel steps due to the sublimation process can be excluded straightaway, since this would lead to energy-dependent (2×1) profiles,¹⁶ which are not observed. In addition, no time-dependent oscillating behavior of the (2×1) spots was observed as found for the integer-order spots due to layer-by-layer sublimation above 270 °C.¹⁶ The splitting must thus stem from parallel and almost regularly spaced antiphase boundaries that have spontaneously formed between translational domains of the (2×1) ordered phase.¹⁷

In order to determine the average distance $\langle L \rangle$ between these antiphase boundaries and the corresponding standard deviation σ , fits to the profiles along the $[110]$ direction were performed using a superposition of two Lorentzians: $I(k_{\parallel}) = I_1(k_{\parallel}) + I_2(k_{\parallel})$, with $I_{1/2}(k_{\parallel}) = \bar{I}_{1/2} \{ 1 + [(k_{\parallel} \pm k_0) / \kappa]^2 \}^{-1}$ and adjustable parameters $\bar{I}_{1/2}$, k_0 , and κ . As described in detail in Ref. 17, this profile shape corresponds to a geometric distribution of the domain width L , which is found to be well justified here because of the excellent agreement of the fit and the experimental data in Fig. 3(a). We thus derive that $\langle L \rangle = 4/\kappa$ (Ref. 17) increases from 18 to 26 Å for temperatures of 270 and 340 °C, while values of $\sigma/\langle L \rangle$ change from 0.72 to 0.78. Evidently, the fluctuation of L is rather broad.

On the basis of this result we propose a structural model of the observed antiphase boundaries [Fig. 3(b)]. It accounts for the (antiphase) displacement of the adjacent (2×1) domains by one lattice constant along the $[1\bar{1}0]$ direction and contains a row of additional Cd vacancies at the domain boundary to account for the Cd deficiency of the surface. Such domain boundaries between (2×1) ordered domains can be termed *light* domain walls (DW's), because they exhibit a lower local Cd coverage than the (2×1) domains. This specific type of DW is also supported here from the observed temperature dependence of $\langle L \rangle$ in correlation with the change of the Cd coverage θ_{Cd} in the top layer deduced from the Auger data. From the structure model, θ_{Cd} is calculated as $\theta_{\text{Cd}} = 0.5(1 - a/\langle L \rangle)$ ML (a being the surface lattice constant of 4.58 Å), which yields $\theta_{\text{Cd}} = 0.37$ ML at 270 °C and 0.41 ML at 340 °C, using the experimentally determined values of $\langle L \rangle$. Calibrating the coverage deduced from the Auger ratio at 270 °C to 0.37 ML [see Fig. 2(b)], the θ_{Cd} value derived from the Auger data at 340 °C, is in excellent agreement with $\theta_{\text{Cd}} = 0.41$ ML, as expected on the basis of the DW model, thus giving further evidence for it.

The most plausible reason for the formation of such DW's is the reduction of surface strain. Due to its symmetry, the (2×1) phase does not allow an effective relaxation of the surface strain by bond rotations around the Cd atoms of the third layer, as it is possible for the $c(2 \times 2)$ phase.⁶ As a consequence, the binding geometry of the second-layer Te atoms to the third-layer Cd atoms cannot preserve the tetrahedral angles as in the $c(2 \times 2)$ phase. A considerable surface strain along the $[110]$ direction is therefore expected. Since the DW's break the twofold surface symmetry, they constitute sites for strain relief by the locally different surface geometry.

The average distance $\langle L \rangle$ between the DW's is determined by the strain relief in the domain cores, and by the energy required for the formation of the DW's with respect to the ideal (2×1) reconstruction. The short spacing of 4–6 lattice constants indicates a rather strong surface strain in the (2×1) phase. At higher temperatures the surface strain appears to diminish slightly, possibly due to a small thermal expansion of the bulk lattice and/or to relief of the surface strain by excitation of transverse surface phonons, leading to the increase of $\langle L \rangle$. The most important aspect is, however, that the presence of the DW's lowers the free energy of the (2×1) phase with respect to that of the $c(2\times 2)$ phase and thus causes the phase transition to occur at a lower temperature than it would without formation of DW's.

To our knowledge, no such observation of a temperature-driven formation of DW's in a binary semiconductor surface has been reported previously. Nevertheless, this scenario observed for the CdTe(001) surface is expected to be meaningful for other binary semiconductor surfaces, too. For instance, one may speculate that on the As-terminated GaAs(001) surface, a similar formation of DW's is responsible for the anti-phase disorder at the temperature-driven $c(2\times 8)-(2\times 4)$ phase transition, which is similar from the viewpoint of symmetry.¹⁸

Concerning the CdTe(001) surface, several important implications arise. First of all, the results indicate that vacancies in the top layer may already be energetically favored under equilibrium conditions at higher temperatures, since by formation of DW's they offer a mechanism by which the surface can reduce its strain. Secondly, the important role of the DW's derived for the (2×1) phase illustrates that theoretical predictions of the most stable surface reconstructions, based on comparisons of *ideal* reconstructions, may be misleading, especially when energy differences of the ideal reconstruc-

tions (as mentioned) are small.⁴ A third important point is the implication of the observed DW's for desorption and growth processes. Evidently, the DW's constitute a preferential site for the nucleation of vacancy islands during sublimation and can thus reduce the corresponding effective activation energies.^{15,19} The DW's should also play a key role for the understanding of the surface morphology during ion ablation of CdTe(001), for which strongly anisotropic islands have been observed.²⁰ Finally, the presence of DW's probably answers a long-standing question for the CdTe(001) surface, namely, why a $c(2\times 2)$ phase is observed under external Cd flux, e.g., under growth conditions, whereas a (2×1) phase is found under UHV at the same temperatures.⁵ The reason is most likely that the DW's are annihilated by the high concentration of Cd atoms on the surface due to the external flux, which causes a high surface strain of the (2×1) phase, thus making the $c(2\times 2)$ phase energetically more stable, even at temperatures above the UHV phase transition temperature ($\geq 270^\circ\text{C}$).

In summary, from high-resolution low-energy electron diffraction data we have deduced the formation of parallel domain walls in the (2×1) phase at the temperature-driven $c(2\times 2)-(2\times 1)$ phase transition of the CdTe(001) surface. These are formed by spontaneous ordering of Cd surface vacancies and lower the surface strain in the (2×1) reconstruction. This type of phase transition has to be expected for other (001) surfaces of binary semiconductors, too, and has important implications for several of their properties.

We thank Professor E. Umbach for his stimulating support and a critical reading of the manuscript and Dr. V. H. Etgens, Dr. C. Heske, and Dr. J. Wollschläger for fruitful discussions. This work was supported by the Deutsche Forschungsgemeinschaft through SFB 410.

*Corresponding author. Email address: sokolowski@physik.uni-wuerzburg.de

¹J. Moison, C. Guille, and M. Bensoussan, Phys. Rev. Lett. **58**, 2555 (1987).

²D. Martrou, J. Eymery, and N. Magnea, Phys. Rev. Lett. **83**, 2366 (1999).

³A. R. Avery, C. M. Goringe, D. M. Holmes, J. L. Sudijono, and T. S. Jones, Phys. Rev. Lett. **76**, 3344 (1996).

⁴S. Gundel, A. Fleszar, W. Faschinger, and W. Hanke, Phys. Rev. B **59**, 15 261 (1999).

⁵S. Tatarenko, B. Daudin, D. Brun, V. H. Etgens, and M. B. Veron, Phys. Rev. B **50**, 18 479 (1994).

⁶M. B. Veron, M. Suvage-Simkin, V. H. Etgens, S. Tatarenko, H. A. Van Der Veegt, and S. Ferrer, Appl. Phys. Lett. **67**, 3957 (1995).

⁷L. Seehofer, G. Falkenberg, R. L. Johnson, V. H. Etgens, D. Brun, and B. Daudin, Appl. Phys. Lett. **67**, 689 (1995).

⁸C. Heske, U. Winkler, G. Held, R. Fink, E. Umbach, Ch. Jung, P. R. Bressler, and Ch. Hellwig, Phys. Rev. B **56**, 13 335 (1997).

⁹M. Schick, Prog. Surf. Sci. **11**, 245 (1981).

¹⁰H. Neureiter, S. Spranger, M. Schneider, U. Winkler, M. Sokolowski, and E. Umbach, Surf. Sci. **388**, 186 (1997).

¹¹W. Ranke and K. Jakobi, Surf. Sci. **63**, 33 (1977).

¹²H. Neureiter, Ph.D. thesis, Universität Würzburg, 1998.

¹³D. Martrou, J. Eymery, P. Gentile, and N. Magnea, J. Cryst. Growth **184/185**, 203 (1998); (private communication).

¹⁴J. Cibert and S. Tatarenko, Defect Diffus. Forum **150-151**, 1 (1997).

¹⁵S. Tatarenko, B. Daudin, and D. Brun, Appl. Phys. Lett. **65**, 734 (1994).

¹⁶H. Neureiter, M. Schneider, S. Tatarenko, M. Sokolowski, and E. Umbach, Appl. Surf. Sci. **123**, 71 (1998).

¹⁷J. Wollschläger, Surf. Sci. **383**, 103 (1997).

¹⁸J. M. Van Hove, P. Cohen, and C. S. Lent, J. Vac. Sci. Technol. A **1**, 546 (1983).

¹⁹S. Krishnamurthy, M. A. Berding, A. Sher, and A.-B. Chen, Phys. Rev. Lett. **64**, 2531 (1990).

²⁰V. H. Etgens, R. M. Ribeiro-Teixeira, P. M. Mors, M. B. Veron, S. Tatarenko, M. Sauvage-Simkin, J. Alvarez, and S. Ferrer, Europhys. Lett. **36**, 271 (1996).